

Chromatic dispersion effect in a microwave photonic filter using superstructured fiber Bragg grating and dispersive fiber

Wei Zhang, Ian Bennion and John A. R. Williams

Photonics Research Group, Department of Electrical Engineering, Aston University, Birmingham, B4 7ET, UK
w.zhang@aston.ac.uk

Abstract: In this paper a microwave photonic filter using superstructured fiber Bragg grating and dispersive fiber is investigated. A theoretical model to describe the transfer function of the filter taking into consideration the spectral width of light source is established. Experiments are carried out to verify the theoretical analysis. Both theoretical and experimental results indicate that due to chromatic dispersion the source spectral width introduces an additional power penalty to the microwave photonic response of the filter.

©2005 Optical Society of America

OCIS codes: (070.6020) Signal processing; (060.2430) Fibers, single-mode; (060.2340) Fiber optics components.

References and links

1. B. Moslehi, J. W. Goodman, M. Tur, and H. J. Shaw, "Fibre-optic lattice signal processing," *Proc. IEE* **72**, 909-930 (1984)
2. R. A. Minasian, "Photonic Signal Processing of High-Speed Signals Using Fibre Gratings," *Opt. Fiber Technol.* **6**, 91-108 (2000)
3. B. A. L. Gwandu, W. Zhang, J. A. R. Williams, L. Zhang, and I. Bennion, "Microwave photonic filtering using Gaussian-profiled superstructured fibre Bragg grating and dispersive fibre," *Electron. Lett.* **38**, 1328-1330, (2002)
4. J. S. Leng, W. Zhang and J. A. R. Williams, "Optimisation of superstructured fibre Bragg gratings for microwave photonic filters response," *IEEE Photonics Technol. Lett.* **16**, 1736-1738 (2004)
5. H. Schmuck, "Comparison of optical millimetre wave system concepts with regard to chromatic dispersion," *Electron. Lett.* **31**, 1848-1849 (1995)
6. G. J. Meslener, "Chromatic dispersion induced distortion of modulated monochromatic light employinh direct detection," *IEEE J. Quantum Electron.* **20**, 1208-1216 (1984)
7. W. Zhang, J. A. R. Williams and I. Bennion, "Analysis of Frequency Response of a Microwave Photonic Filter using Superstructured Fiber Bragg Grating," in *Proceedings of 17th Annual Meeting of the IEEE-Lasers-and-Electro-Optics-Society*, (Porto Rico, 2004), pp. 276-277.
8. D. Marcuse, "Pulse distortion in single-mode fibers," *Appl. Opt.*, **19**, 1653-1660 (1980)

1. Introduction

The advantages of microwave photonic systems have been recognized and such systems are currently being considered for a number of applications including personal communications networks, millimeter-wave radio LANs, broadband video distribution networks and signal distribution for phased array antennas.

Signal processing is a key operation in all those systems. The advantages including reduced size and weight, low and constant attenuation over the entire modulation frequency range, imperviousness to electromagnetic interference, wide bandwidth, low dispersion and high information transfer capacity etc, can be accumulated by performing microwave signal processing using optical techniques, preferably with fiber-optic compatible components. There has been much effort in this area and a large number of configurations have been reported [e.g., 1]. More recently the development of fiber Bragg gratings has lead to numerous

applications in microwave photonic signal processing [e.g. 2]. Since fiber Bragg gratings own the advantages of ease and accuracy in imprinting on fiber and controllable spectral response, it provides a compact versatile device for use in this application and enable the development of more complex signal processing functions and better filtering performance.

A microwave photonic filter using Superstructured fiber Bragg grating (SFBG) and dispersive fiber was first proposed in [3]. In such a structure time delays between optical taps are determined by the product of wavelength spacing of adjacent optical reflections and the dispersion introduced by the fiber, therefore precisely matched to produce higher rejection level [3][4]. The distortion in the filters' responses happens at high frequencies, which is as attributed to the power degradation caused by fiber chromatic dispersion, although the theoretical simulations based on the well-known analysis [5] do not match well to the experimental results in [3][4].

In the theoretical analyses of power degradation caused by fiber chromatic dispersion in [5][6] a monochromatic optical carrier source is assumed. However, in a microwave photonic filter using a superstructured fiber Bragg grating the effect of the source spectral width cannot be ignored. We have presented a primary result in [7]. In this paper we further the investigation of the frequency response of a microwave photonic filter utilizing a superstructured fiber Bragg grating in a greater detail. A strict theoretical model is first established to describe the transfer function of dispersive fiber when using a light source with limited spectral width, and an analytical expression is obtained. A microwave photonic filter is constructed using SFBGs and 25 km/50 km of standard single mode fiber to experimentally investigate the microwave photonic response. Results demonstrate that the spectral width of the light source introduces an extra power penalty that is exponentially related to the square of the product of the source spectral width, fiber dispersion and modulation frequency.

2. Theory

In an intensity-modulated system, the modulated light wave can be expressed as,

$$\begin{aligned}\psi(t) &= f(t)\psi_0(t) \\ &\approx [I_0 + I_1 \cos(\Omega t)]\psi_0(t)\end{aligned}\quad (1)$$

for either using direct modulation or an external optical modulator. Here $f(t)$ represents the modulation function, $\psi_0(t)$ is the unmodulated optical field, Ω the fundamental modulation frequency. For a linear modulation it consists of DC and fundamental frequency components, and I_0, I_1 are the amplitudes of DC and fundamental frequency modulation, respectively. For systems using an external optical modulator that is mostly employed for broadband modulation, (1) can be written as [5][6],

$$\psi(t) \approx [J_0(m) - 2J_1(m) \cos(\Omega t)]\psi_0(t) \quad (2)$$

where $J_0(\cdot), J_1(\cdot)$ are zero and the first order Bessel function of the first kind, respectively, and m is the modulation index. For simplicity we assume that modulation process does not affect the phase of the light wave. The amplitude spectrum of a light source is obtained by the Fourier transform,

$$\begin{aligned}\phi(\omega) &= \frac{1}{2\pi} \int_{-\infty}^{\infty} \psi(t) \exp(-i\omega t) dt \\ &= \frac{1}{2\pi} \int_{-\infty}^{\infty} \psi_0(t) f(t) \exp(-i\omega t) dt \\ &= \int_{-\infty}^{\infty} \phi_0(\omega') F(\omega - \omega') d\omega'\end{aligned}\quad (3)$$

where $\phi_0(\omega)$ and $F(\omega)$ are the Fourier transforms of $\psi_0(t)$ and $f(t)$, respectively. The amplitude of a light wave travelling in the fiber with propagation constant β can be expressed by means of the Fourier transform of its spectrum $\phi(\omega)$,

$$\psi(z, t) = \int_{-\infty}^{\infty} \phi(\omega) \exp[i(\omega t - \beta z)] d\omega \quad (4)$$

where z is the travel distance in the fiber.

The ensemble average of the power $|\psi(z, t)|^2 = P(z, t)$ can be expressed in terms of the autocorrelation function of the spectrum as follows [8]:

$$\langle P(z, t) \rangle = \int_{-\infty}^{\infty} |\hat{\phi}_0(\omega_0 - \omega')|^2 \cdot \left| \int_{-\infty}^{\infty} F(\omega - \omega') \exp\{i[(\omega - \omega')t - (\beta - \beta')z]\} d\omega \right|^2 d\omega' \quad (5)$$

where $|\hat{\phi}_0(\omega)|^2$ is the spectral density function of the light source. We expand the propagation constant β as a function of the frequency difference $\omega - \omega_0$, where ω_0 is the central angular frequency of the light source,

$$\beta = \beta_0 + \dot{\beta}_0(\omega - \omega_0) + \frac{1}{2}\ddot{\beta}_0(\omega - \omega_0)^2 + \dots \quad (6)$$

β_0 is the propagation constant at the central angular frequency, the dot indicates differentiation with respect to ω .

With the help of (2) and (6) we can first solve the integral of $d\omega$.

$$\begin{aligned} \eta(\omega') &= \int_{-\infty}^{\infty} F(\omega - \omega') \exp\{i[(\omega - \omega')t - (\beta - \beta')z]\} d\omega \\ &= \int_{-\infty}^{\infty} \{J_0(m)\delta(\omega - \omega') - J_1(m)[\delta(\omega - \omega' - \Omega) + \delta(\omega - \omega' + \Omega)]\} \exp\{i[(\omega - \omega')t - (\beta - \beta')z]\} d\omega \\ &= J_0 - J_1 \cos\{\Omega t - \Omega z[\dot{\beta}_0 + \ddot{\beta}_0(\omega' - \omega_0)]\} \exp(-i\frac{1}{2}\ddot{\beta}_0\Omega^2 z) \end{aligned} \quad (7)$$

where the propagation constant derivatives higher than the second order have been neglected. The square of the modulus is

$$\begin{aligned} |\eta(\omega')|^2 &= J_0^2 - 2J_0J_1 \cos\{\Omega t - \Omega z[\dot{\beta}_0 + \ddot{\beta}_0(\omega' - \omega_0)]\} \cos(\frac{1}{2}\ddot{\beta}_0\Omega^2 z) \\ &\quad + J_1^2 \cos^2\{\Omega t - \Omega z[\dot{\beta}_0 + \ddot{\beta}_0(\omega' - \omega_0)]\} \end{aligned} \quad (8)$$

A good approximation to most spectral density functions of the light source is the Gaussian function

$$|\hat{\phi}_0(\omega_0 - \omega)|^2 = \frac{P_0}{\pi^{1/2}W} \exp[-(\omega - \omega_0)^2 / W^2] \quad (9)$$

with energy P_0 and spectral width $2W$. Using the above outcome then we can calculate (5) as,

$$\begin{aligned} \langle |P(z, t)|^2 \rangle &= \int_{-\infty}^{\infty} \frac{P_0}{\pi^{1/2}W} \exp[-(\omega' - \omega_0)^2 / W^2] |\eta(\omega')|^2 d\omega' \\ &= P_0 \{J_0^2 + \frac{1}{2}J_1^2 + 2J_0J_1 \exp[-(\frac{W\ddot{\beta}_0\Omega z}{2})^2] \cos(\frac{\ddot{\beta}_0\Omega^2 z}{2}) \cos[\Omega(t - \dot{\beta}_0 z)] \\ &\quad + \frac{1}{2}J_1^2 \exp[-(W\ddot{\beta}_0\Omega z)^2] \cos[2\Omega(t - \dot{\beta}_0 z)]\} \end{aligned} \quad (10)$$

The term associated with the fundamental modulation frequency Ω in (10) is chosen to simulate the output response, as not only the second harmonic is weak but also the components other than the one with fundamental frequency is not detected when a lightwave component analyzer (or network analyzer) is used. Therefore the detected signal can be expressed as,

$$I|_{\Omega} \propto 2P_0J_0J_1 \exp[-(\frac{W\ddot{\beta}_0\Omega z}{2})^2] \cos(\frac{\ddot{\beta}_0\Omega^2 z}{2}) \quad (11)$$

From the above expression it is clear that for a monochromatic source when the spectral width $2W$ reduces to zero the measured response can then be proportional to $\cos(\frac{\ddot{\beta}_0\Omega^2 z}{2})$, which is a well known expression [5]; for a source with limited spectral width, there is an

extra factor that is the function of the source spectral width, modulation frequency and fiber length. This factor causes dispersion effects to take place attenuating the detected signal in frequency domain much faster than that of only using a monochromatic source.

3. Microwave photonic filter using superstructured fiber grating and dispersive fiber

The reflection spectrum of a typical SFBG is shown in Fig. 1, consisting of several optical channels. If light wave with this spectral profile is launched into dispersive medium such as a chirp-Bragg grating or dispersive fiber, these channels will experience differential time delays. Such a device can thus generate a series of optical taps with a unit time delay determined by the product of the wavelength spacing and the dispersion introduced by the medium.

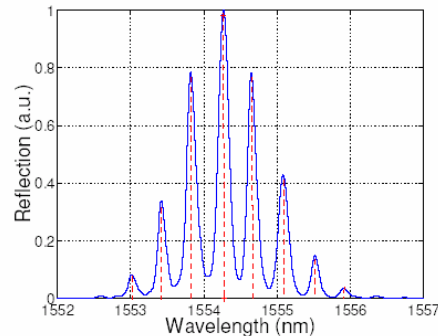


Fig. 1. Measured optical reflection spectrum of a superstructured Bragg grating.

The basic arrangement to realize a microwave photonic bandpass filter is shown in Fig. 2. The light from a broadband light source is launched through a circulator, reflected by a superstructured fiber grating and modulated via an electro-optic modulator, then coupled into a fiber link, detected and analyzed by a Lightwave Component Analyzer. An erbium doped fiber amplifier (EDFA) is used to compensate for the optical loss in the system. The superstructured fiber grating slices the broadband source, producing a source with the spectrum as shown in Fig. 1. From the optical spectrum we can see that it consists of 8 significant channels with a spacing of ~ 0.41 nm and channel spectral widths of 0.12 nm.

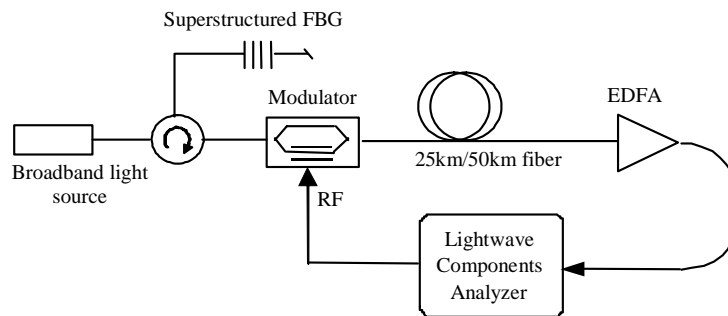


Fig. 2. Diagram of the microwave photonic filter using SFBG and dispersive fiber.

4. Results and discussion

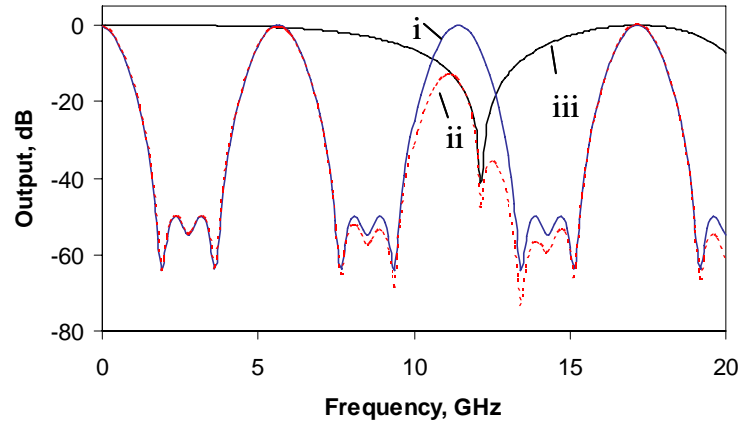


Fig. 3. Simulated responses without considering the source spectral width. i: ideal 8-tap response, ii: 8-tap response of 25km fiber, iii: 1-tap response of 25km fiber.

For an ideal 8-tap bandpass filter with tap weights represented by channel peak reflection (as indicated by the dotted lines in Fig. 1) the simulated response is shown as trace 'i' in Fig. 3. For a filter with such 8 taps and 25 km of standard single mode fiber, the synthesized microwave response can be simulated based on the analysis of [3], depicted as trace 'ii' in Fig. 3 where the spectral width has been considered as infinitesimal. This would be the case when 8 narrow linewidth lasers with a 0.41nm wavelength spacing are used. Since the time delays between the different taps are introduced by the fiber dispersion experienced by the taps with different wavelengths the carrier suppression occurs in the frequency response of the filter. Comparing 'ii' with 'i' it is clear that the filter response is distorted by the dispersion effect and the envelope of trace 'ii' exactly follows trace 'iii' in Fig. 3, which is the response of 25 km of fiber using a single monochromatic source (1 tap).

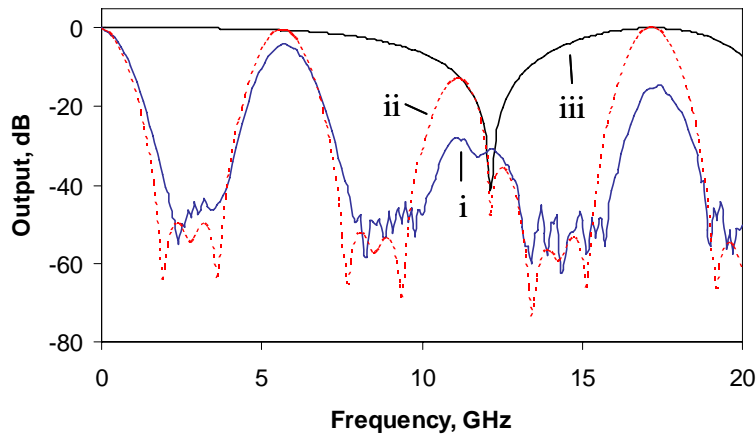


Fig. 4. Measured and simulated responses of 25km fiber. i: measured 8-tap response, ii: simulated 8-tap response with zero source spectral width, iii: 1-tap response with zero source spectral width.

When an optical spectrum-sliced light source is used the source spectral width cannot be treated as infinitesimal. The experiment was carried out by measuring the response of the filter using the SFBG and 25 km of fiber. The measured response of the filter is depicted as

trace 'i' in Fig. 4 while the theoretical responses of the filter is simulated and shown as trace 'ii', which assumes the infinitesimal channel spectral width. The response of 25km fiber using a single monochromatic source is also depicted as trace 'iii'. Comparing 'i' with 'ii' we can notice that a large difference exists between the measured response and the simulated response where the source spectral width is ignored. In the measured result the passband responses at higher frequencies are more distorted and reduced than the simulated results. Especially at around 12 GHz where the passband response is much lower than the simulation. It is obvious that the analysis which ignores the source spectral width cannot describe the frequency response of the filter.

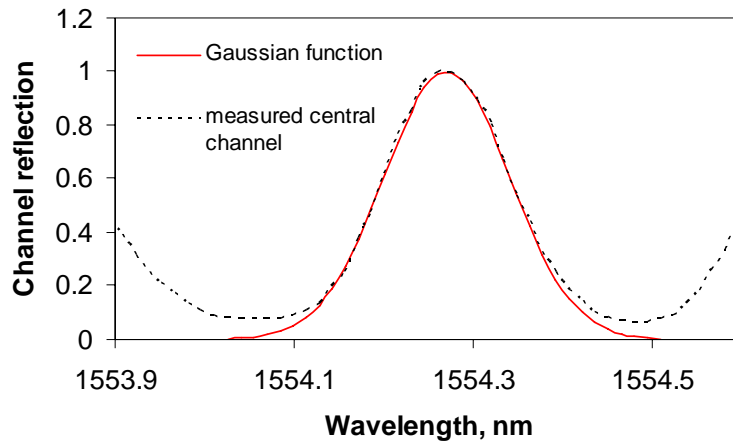


Fig. 5. Optical spectra of the central reflection channel of an SFBG

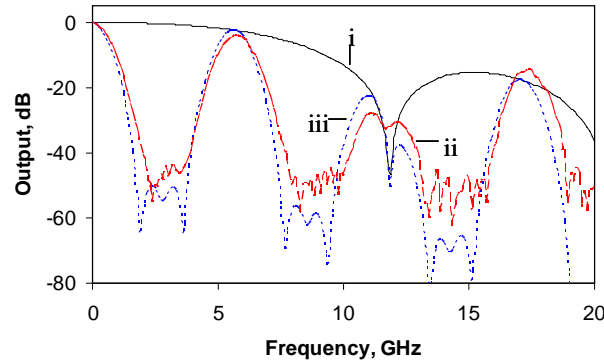


Fig. 6. Measured and simulated responses of 25km fiber in consideration of a spectral width of 0.12 nm. i: simulated 1-tap response, ii: measured 8-tap response, iii: simulated 8-tap response.

Based on Eq. (11) obtained in our theoretical analysis we re-calculated the frequency response of the filter by considering each channel of the SFBG with a Gaussian spectral density function. It should be pointed out that all the gratings used in the experiments are weak gratings in order to ensure the source has a Gaussian spectral density function. It is well known that in a weak grating the reflectivity can be treated as the Fourier transform of coupling coefficient distribution along the grating [4]. Generally a Gaussian apodisation function is used to suppress sidelobes in the grating reflection. The Fourier transform of a Gaussian function still is a Gaussian function. Therefore Gaussian-apodised weak gratings produce a reflection with Gaussian spectral profiles, as does each channel in a Gaussian-

apodised SFBG since the multiple channels of SFBG are the duplicates of the central channel at the harmonics of sampling period [3]. The optical spectrum of the central channel of the SFBG defined by Fig. 1, and theoretical spectrum described by the Gaussian function are presented in Fig. 5. As can be seen there is a good approximation.

We first assume that the light from a single channel with a spectral width of 0.12 nm is launched into 25km of single mode fiber, the response of which is calculated and shown as trace 'i' in Fig. 6. Clearly, the calculated curve is approaching the envelope of the measured trace 'ii'. We then calculated this 25km fiber's response by using 8 optical taps, each with 0.12nm spectral width to approximate the actual source spectrum shown in Fig. 1. The calculated result is shown as trace 'iii' in Fig. 6. Now we can see that this calculated response is in reasonable agreement with the measured one. Comparing Fig. 6 with Fig. 4, clearly Eq. (11) provides much better description of fiber dispersion effect in such a system.

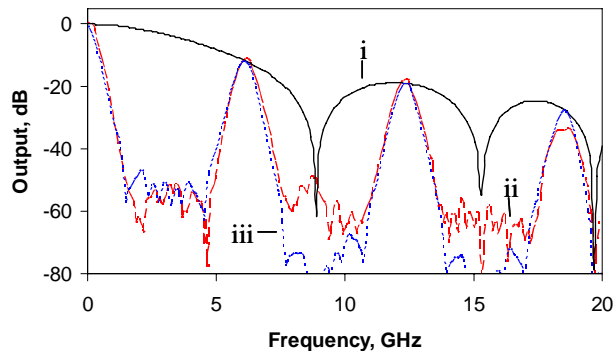


Fig. 7. Measured and simulated responses of 50 km fiber in consideration of a spectral width of 0.09 nm. i: simulated 1-tap response, ii: measured 8-tap response, iii: simulated 8-tap response.

Another filter's response was also measured and calculated. Figure 7 shows both theoretical and experimental responses of a filter using 50 km of single mode fiber and a superstructured fiber grating with channel spacing of 0.21 nm and channel spectral width of 0.09 nm. Fig. 7 shows a better agreement between experiment and simulation.

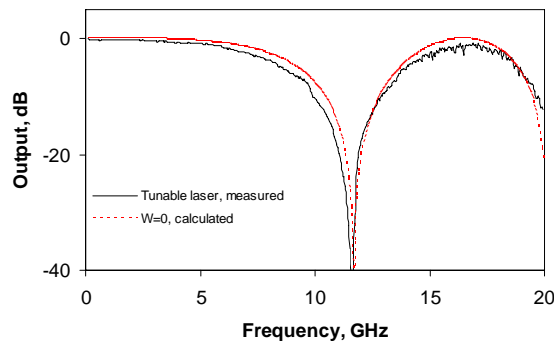


Fig. 8. Measured and simulated 1-tap responses of 25 km fiber.

It should be pointed out that there still are some differences between the measured and simulated responses. These differences can be considered as the contribution of several factors. Firstly, due to the imperfection of fiber grating, not all the reflection channels of the SFBG can be well approximated by a Gaussian function. Secondly, a single channel width used in the simulation may not represent the true situation, especially for the weaker channels; thirdly and most importantly, in the beginning of the theoretical analysis we have assumed that the modulation process does not affect the phase of the light wave, which is an ideal case. In

practice this can not be true. Either direct modulation or an external modulator introduces frequency chirp, implying that a slight frequency or phase modulation is parasitic in the modulated light wave signal and will certainly contribute to the resultant microwave photonic response. This can be seen from the comparison of measured and simulated 1-tap response of the 25 km fiber (Fig. 8) where the factors of source spectral shape and width have been excluded (the tunable laser used in the measurement has a linewidth of 100 kHz), however, there still exists some disagreement between measured and theoretical responses due to the frequency chirp.

The phase of the light source certainly contributes to the resultant response. For the source with limited spectral width the phase turns out to be a high frequency noise. This feature, however, has been considered and statistically characterised by the optical spectrum density function in the theoretical analysis. For most light sources the statistic density of phase noise has a Gaussian distribution thus most light sources have a Gaussian spectral density function. In the experiments of this work all the gratings were designed to produce optical reflections with a near Gaussian spectral shape.

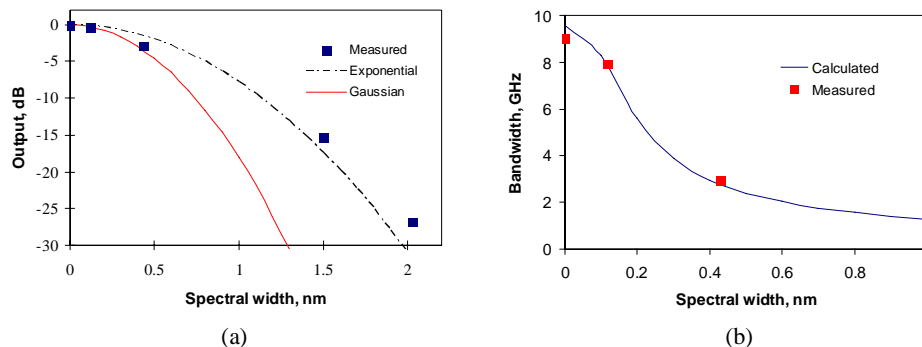


Fig. 9. (a) Filter output at fixed frequency vs. source spectral width. (b) Operational bandwidth vs. source spectral width.

The one-tap response of the 25km fiber was investigated under different source spectral width. One tunable laser, 2 weak fiber Bragg gratings and 2 optical bandpass filters, which have spectral widths of 100 kHz, 0.12 nm, 0.43 nm, 1.5 nm and 2.03 nm respectively, were used to slice the broadband light source. Response levels at a fixed frequency (here 2GHz) were measured and are plotted against spectral width in Fig. 9(a). The calculated response curve based on Eq. (11) is depicted in Fig. 9(a) as a comparison. It can be seen that the first three measured responses, which are the results of using the laser and two weak gratings, follow the curve calculated by using a Gaussian function as the source spectral distribution; the responses of using 2 optical bandpass filters are closer to another curve, which is calculated by using an exponential function, $\exp(-|\omega-\omega_0|/2W)$, which better matches the spectral responses of optical bandpass filters, as source spectral density function. Obviously the disagreement between the measured and calculated responses strongly depends on the mismatch between the real source spectral shape and the spectral distribution function used in the simulation.

The effect of the source spectral width can greatly reduce the operational frequency range of a microwave photonic filter, which usually is limited by the first notch frequency of the 1-tap response. The relationship between operational bandwidth of a filter and the source spectral width is calculated based on the 1-tap response of the 25km fiber and shown in Fig. 9(b) while a Gaussian spectral density function is assumed. The measured values at 3 different spectral widths are depicted on it as well. From it one can see that the available bandwidth is no longer decided by the first notch frequency and decreases rapidly with the increase of source spectral width.

All the disagreements between measured and calculated results can be removed by taking account of the measured optical spectral response of a sliced light source and the frequency chirp of the modulator in the simulation. In this case, however, closed-form expressions like equations (10) and (11) may not be obtained unless optical spectral response and frequency chirp can be expressed with some simple functions. Although complex numeric calculation can provide the solution, it is beyond the scope of this paper.

5. Conclusion

We have theoretically analyzed and experimentally demonstrated that the effect of the source spectral width introduces an extra power penalty that is exponentially related to the square of product of the source spectral width, fiber dispersion and modulation frequency further reduces the operational bandwidth of such a microwave photonic filter and distorts the frequency response. The experiments on 25/50 km fiber link were carried out using sliced optical sources. The achieved result can be used not only in designing microwave photonic filters but also has implications for the applications of optical spectrum-sliced sources in signal generation and transmission.